



Contents lists available at ScienceDirect

International Journal of Electronics and Communications (AEÜ)

journal homepage: www.elsevier.com/locate/aeue



Regular Paper

CPW bandpass filters with controllable passbands

Jian-Kang Xiao^{a,b,*}, Yong Li^a, Ning Zhang^a, Jian-Guo Ma^c

^aSchool of Electro-Mechanical Engineering, Xidian University, Xi'an 710071, China

^bState Key Laboratory of Millimeter Waves, Nanjing 210096, China

^cTianjin University, Tianjin 300072, China

ARTICLE INFO

Article history:
 Received 11 September 2015
 Accepted 6 May 2016
 Available online xxxxx

Keywords:
 Coplanar waveguide (CPW)
 Bandpass filter (BPF)
 Dual-band
 Tri-band

ABSTRACT

Defected coplanar waveguide (CPW) resonator has been analyzed, and multi-band bandpass filters with individually controllable passband have been developed. New dual-band and tri-band bandpass filters which center at 2.4/3.5/5.2 GHz have been designed, fabricated and measured. The measurements demonstrate the new presentations. The measured filter passband insertion losses are less than 2.7 dB. It has been noticed that the filter center frequencies can be individually controlled, and the bandwidths can be individually adjusted. Advantages of the new design are not only its simple and compact circuit topology, miniature circuit size, but also its less electromagnetic leakage.

© 2016 Elsevier GmbH. All rights reserved.

1. Introduction

Coplanar waveguide circuits have important applications in microwave systems because of the outstanding virtues of easy integration with the lumped elements and other microwave components. In this research, it has been noticed that when there are etched patterns or slots in the CPW conductor strip, the electromagnetic field distributions may be changed, and resonances may be introduced when the electric field and the magnetic field keep balance. In order to control each passband of the multi-band bandpass filter independently, a design scheme is presented. In this scheme, (1) etched patterns with different length generate different resonances; (2) each pattern only needs generating a single resonance in order to control each passband effectively. It has been demonstrated that the individually controllable resonances can be easily obtained by the etched patterns, and the other assistance such as microstrip resonators or CPW ground resonators are not required. This is very useful for miniature multi-band filter design.

In this paper, coplanar waveguide bandpass filters with dual-band and tri-band have been proposed. Filter center frequency and bandwidth can be easily controlled only by controlling the corresponding etched pattern. Compared with the related reports [1–3], the new CPW filters meet the requirement of more flexible design, more controllable bands, and even smaller dimensions. Compared with the DGS coplanar waveguide bandpass filters

[1,4,5], the new designs have less circuit complexity and less electromagnetic waves leakiness. CPW circuit is more immune than DGS from crosstalk and ground plane interference not only because the conductor strip and the ground are coplane but also because there is no manipulation on the ground plane. The proposed filter design scheme is helpful for multi-band microwave filters design.

2. Analysis of the defected CPW resonator

When there are etched slots/patterns in the CPW conductor strip, resonances can be produced. Fig. 1 shows the defected CPW resonator, where two identical L-shaped slots are etched in the conductor strip. Resonant frequency and bandwidth can be controlled by the etched slots. Equivalent transmission line model that ignores the inner couplings is plotted in Fig. 1(b). According to the transmission line and network theory, each parameter of the ABCD matrix can be expressed as

$$A = \cos \theta_e, \quad B = jZ_b \sin \theta_e \tag{1}$$

$$C = \frac{-jZ_a \cos \theta_a \sin^2 \theta_e - 2Z_b \sin \theta_a \sin \theta_e \cos \theta_e}{Z_a Z_b \cos \theta_a \sin \theta_e} \tag{2}$$

$$D = \frac{Z_a \cos \theta_a \cos \theta_e - 2Z_b \sin \theta_a \sin \theta_e}{Z_a \cos \theta_a} \tag{3}$$

where Z_a , Z_b and Z_d are characteristic impedances of CPW with widths of w_a , w_b and w_d , respectively. Electric length can be expressed as $\theta_i = \omega l_i \sqrt{\epsilon_{re_i}}/c$, $\theta_e = \theta_b + \theta_m$, $\theta_m = \arctan[Z_b/Z_d] \tan \theta_d$. $i = a, b, d$; l_i is the physical length; c is the velocity of light in free

* Corresponding author at: School of Electro-Mechanical Engineering, Xidian University, Xi'an 710071, China.

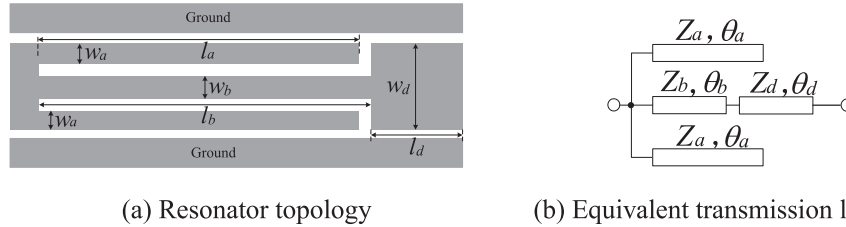


Fig. 1. Defected CPW resonator.

space; ϵ_{re} is the effective permittivity. S_{21} can be expressed with ABCD as $S_{21} = 2/(A + B/Z_0 + CZ_0 + D)$ [6]. When S_{21} equals zero, frequency point of the transmission zero can be computed and predicted as

$$f_z = c(2n + 1)/(4l_a\sqrt{\epsilon_{rea}}), \quad n = 0, 1, 2, \dots \quad (4)$$

Resonant frequency of the CPW resonator can be obtained when S_{21} equals 1, from which the resonant condition can be expressed as

$$(P/Q)^2 + (P/R)^2 = 1 \quad (5)$$

where P , Q and R can be expressed as

$$P = 2Z_0Z_aZ_b \cos \theta_a \sin \theta_e \quad (6a)$$

$$Q = 2Z_0Z_b[\sin \theta_e \cos \theta_0(Z_a \cos \theta_a - Z_0 \sin \theta_a) - Z_b \sin \theta_a \sin^2 \theta_b] \quad (6b)$$

$$R = Z_a Z_b^2 \cos \theta_a \sin^2 \theta_e - Z_0^2 Z_a \cos \theta_a \sin^2 \theta_e \quad (6c)$$

When $l_a = 10.8$ mm, $l_b = 11$ mm, $l_d = 2.5$ mm, $w_a = 0.3$ mm, $w_b = 1.2$ mm, $w_d = 2.2$ mm, it can be calculated by Matlab that the transmission zero and resonant frequency are 2.96 GHz and 2.4 GHz, respectively, which approach to the simulated results of 2.74 GHz and 2.43 GHz.

3. Single band CPW bandpass filter

CPW bandpass filter can be constructed by coupling CPW resonators with wavelength of $\lambda/4$. Defected slots have been introduced in order to control passband effectively, as Fig. 2 shows. Where the four identical L-shaped slots determine the filter center frequency and bandwidth. When designed with second-order ($n = 2$) Chebyshev response with 0.15 dB ripple, the element values of the low-pass prototype are $g_0 = 1$, $g_1 = 0.93$, $g_2 = 0.65$, and $g_3 = 1.43$. The bandpass filter is designed centering at 2.4 GHz with fractional bandwidth (FBW) of 9%. The external quality factor can be obtained as $Q_e = 10.87$. Filter dimensions can be estimated from expressions (5) and (6), the required FBW, and the resonator coupling coefficient, and then are optimized with EM simulator as: $l_1 = 11$ mm, $a_1 = 0.2$ mm, $d_1 = 0.5$ mm, $w = 0.96$ mm, $g = 0.4$ mm, $w_a = 0.3$ mm, $w_b = 1.2$ mm, $w_d = 2.2$ mm. The coupling scheme including the source and load can be formulated by coupling matrix as

$$M = \begin{bmatrix} 0 & -0.0674 & 0 & 0 \\ -0.0674 & 0 & -0.0873 & 0 \\ 0 & -0.0873 & 0 & 0.0623 \\ 0 & 0 & 0.0623 & 0 \end{bmatrix} \quad (7)$$

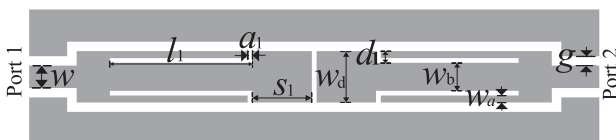


Fig. 2. Topology of the CPW BPF.

The research results on filter center frequency and fractional bandwidth (FBW) variations are illustrated in Tables 1 and 2. The external quality factor can be obtained from $Q_e = f_0/\Delta f_{3dB}$. It indicates that filter center frequency is mainly determined by parameter l_1 , while, bandwidth can be adjusted mainly by etched slot width. Center frequency decreases with l_1 increasing, while, 3 dB bandwidth may increase when slot width increases. Simulated filter frequency responses comparison with l_1 and d_1 are plotted in Fig. 3(a) and (b), respectively, the simulations demonstrate the centre frequency and bandwidth variation rules. Fig. 3(c) shows the comparison of the coupling matrix result and the simulation, the simulated result is similar to the theoretical prediction.

Transmission zeros are attributed to the mixed electromagnetic coupling. It has also been noticed that a longer etched slot can introduce more resonances in a certain frequency band, for which brings more effective capacitance and inductance. But for this case, the required resonances are difficult to control because these resonances are relevancy each other, which limits the multi-band applications. So, individually controlled slots have been introduced for multi-band BPF design in order to obtain individually controllable passbands.

The proposed CPW bandpass filter is different from the traditional CPW filter because the filter performance can be controlled by the etched slots. Simulated electromagnetic field distributions of the CPW bandpass filter are illustrated in Fig. 4(a) and (b). It is seen that the electric field and the magnetic field concentrate on the edge of etched slots with different part, the electric field has stronger magnitude. The current path of the CPW bandpass filter is plotted in Fig. 4(c). The inner coupling of the CPW resonator with etched slots is mixed electromagnetic coupling (MEMC), while, the coupling between neighboring CPW resonators is electric coupling. In this paper, the designs have used ceramic dielectric substrate with a relative permittivity of 10.2 and a thickness of 1.27 mm.

4. Multi-band CPW bandpass filters

4.1. Dual-band CPW BPF

A dual-band CPW bandpass filter with individually controllable passband is proposed. The filter centers at 2.4 GHz and 3.5 GHz with fractional bandwidth of 14.8% and 6.6%, respectively. The passband insertion loss is less than 2 dB. The design procedures: (1) calculate the width of CPW conductor strip, and the width of air gap which is between the conductor strip and the ground, feed lines are set with 50 ohm. (2) Estimate the dimensions of etched slots to meet the desired frequencies. For example, a longer slot and a shorter slot that have been etched in the CPW resonator sat-

Table 1

Filter performance variation versus l_1 , $a_1 = 0.2$ mm, $d_1 = 0.5$ mm, $s_1 = 2.5$ mm.

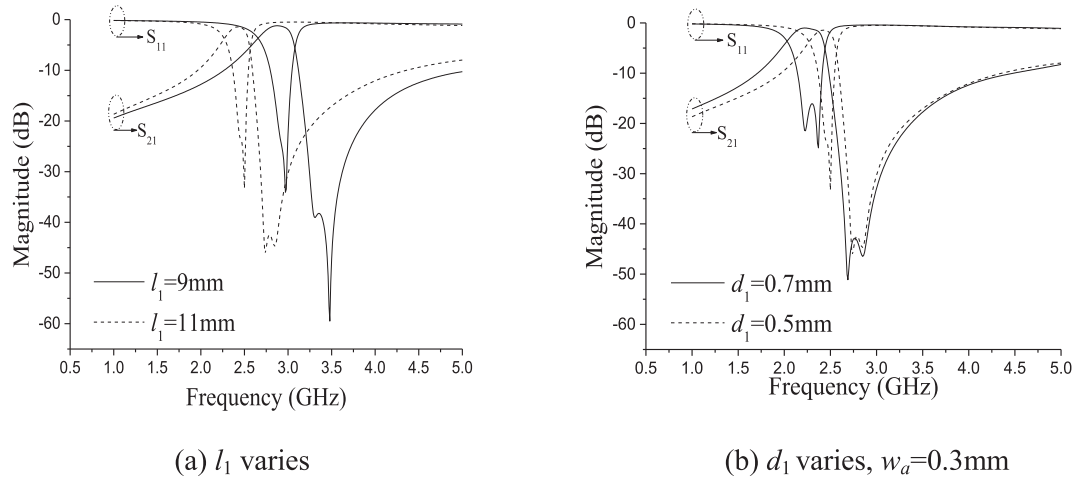
l_1 (mm)	f_0 (GHz)	FBW (%)	Q_e
9.0	2.97	11.4	8.74
10	2.69	10	9.96
11	2.42	9.5	10.87

Table 2
Filter performance variation versus a_1 , $l_1 = 11$ mm, $s_1 = 2.5$ mm, $d_1 = 0.5$ mm.

a_1 (mm)	f_0 (GHz)	FBW (%)	Q_e
0.2	2.42	9.5	10.87
0.4	2.33	14.2	7.06
0.6	2.06	21.4	4.68

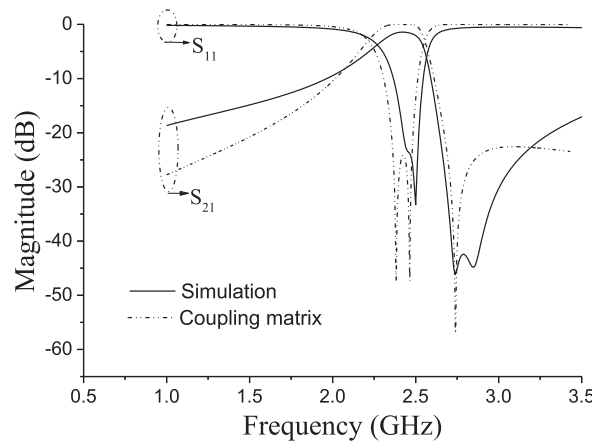
isfy 2.4 GHz and 3.5 GHz, respectively. (3) Determine the width of etched slots to match the desired bandwidth and frequencies. (4) Optimize the design.

The proposed dual-band BPF is plotted in Fig. 5(a), where the filter dimensions are set as: $l_1 = 11$ mm, $l_2 = 6.5$ mm, $a_1 = a_2 = 0.2$ mm, $d_1 = 0.5$ mm, $d_2 = 0.9$ mm, $g = 0.4$ mm, $s_1 = 3$ mm.



(a) l_1 varies

(b) d_1 varies, $w_a = 0.3$ mm



(c) Coupling matrix results and simulated results comparison

Fig. 3. Filter frequency responses comparison.

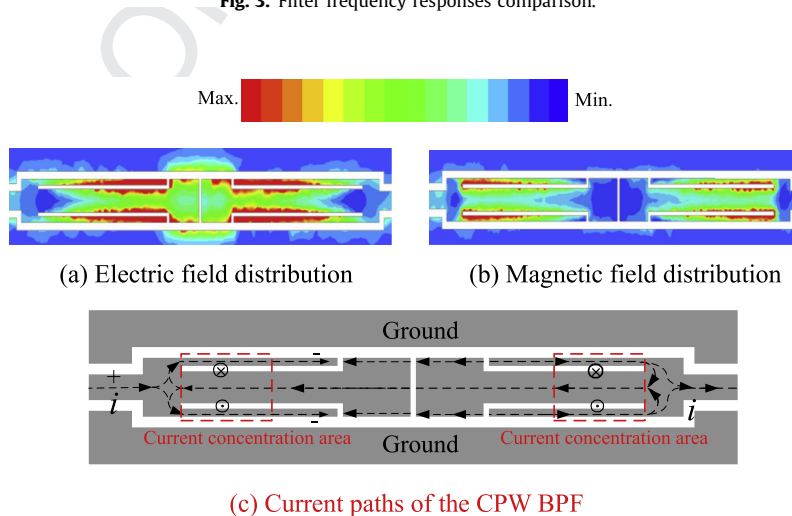


Fig. 4. Filter electromagnetic field distribution at 2.4 GHz and current paths.

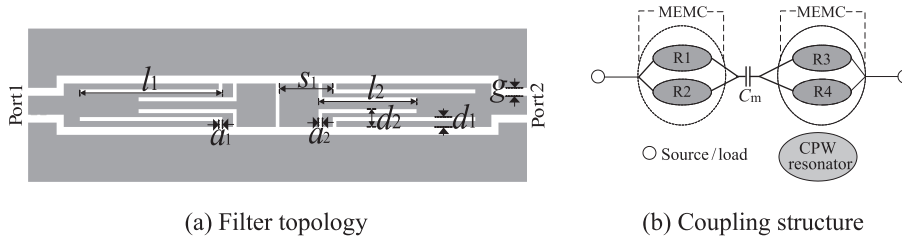


Fig. 5. Dual-band CPW bandpass filter.

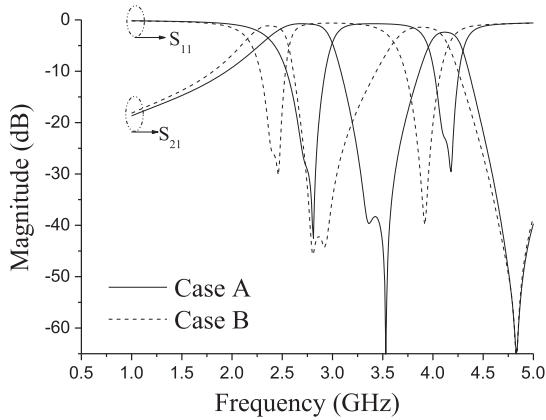


Fig. 6. Dual-band BPF with different center frequencies and bandwidths. Case A: $l_1 = 9$ mm; Case B: $l_1 = 11$ mm.

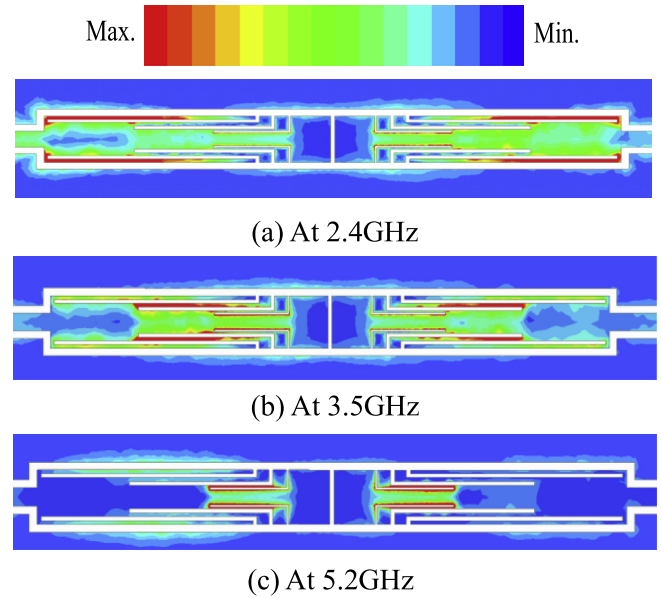
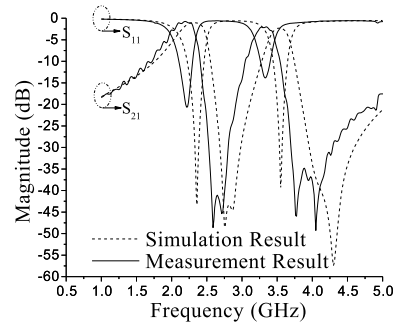
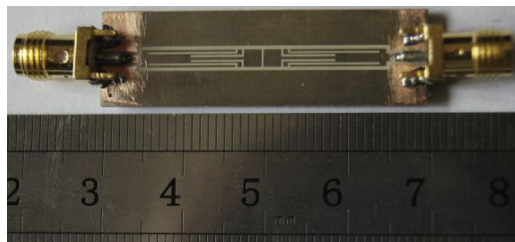


Fig. 9. Simulated current distributions of the tri-band CPW BPF.



(a) Fabricated dual-band CPW BPF (b) Comparison of the simulation and measurement

Fig. 7. Filter fabrication and measurement.

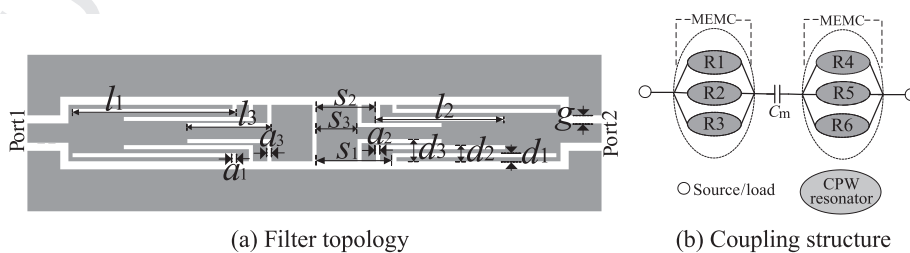


Fig. 8. Tri-band CPW bandpass filter.

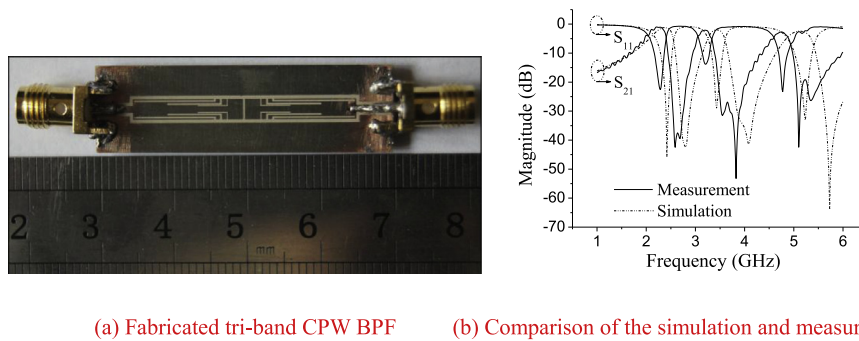


Fig. 10. Filter fabrication and measurement.

Table 3

Performance comparison of this work and other related works.

	Number of passbands	Center frequency (GHz)	Fractional bandwidth (%)	Passband insertion loss (dB)	Passband individually controllable	Complexity	Circuit size (mm ²)
[2]	2	1.8, 2.4	1.7, 1.9	0.14, 0.13	No	High	65 × 0.21
[3]	2	1.575, 2.4	7.5, 4.3	2, 2.6	Yes	High	27 × 22
[7]	1	2.4	12.5	3.5	—	Medium	20 × 17
[8]	2	1.57, 2.4	3, 2	2, 2	No	Low	21.1 × 14.1
This work	2	2.4, 3.5	14.8, 6.6	0.76, 1.98	Yes	Low	40 × 5
	3	2.4, 3.5, 5.2	14.5, 7, 6	1.1, 2.1, 2.7			

The filter coupling scheme is shown in Fig. 5(b), where the etched slots with lengths of l_1 and l_2 can be denoted as resonators R_1 , R_2 , R_3 and R_4 . R_1 – R_3 , R_2 – R_4 are synchronous; while R_1 and R_2 , R_3 and R_4 are asynchronous. The coupling of R_1 – R_3 , and R_2 – R_4 determine the 1st and the 2nd passbands, respectively. The coupling between the two CPW resonators is electric coupling with capacitance of C_m . The filter center frequencies and bandwidths can be individually adjusted by the corresponding slot length and width, respectively. Transmission zeros of the CPW BPF are due to the mixed electromagnetic coupling (MEMC), dominantly the electric coupling.

The center frequencies and bandwidths of the dual-band can be easily adjusted by controlling the corresponding etched slot. Fig. 6 shows the simulated results of the dual-band BPF with different center frequencies and bandwidths. For case A, the filter centers at 2.67 GHz and 4.11 GHz with fractional bandwidth of 21.3% and 4.4%, respectively; For case B, the filter centers at 2.34 GHz and 3.88 GHz with fractional bandwidth of 15.4% and 11.1%, respectively. The proposed dual-band BPF which centers at 2.4/3.5 GHz is fabricated and tested. The fabrication and measurement are shown in Fig. 7(a) and (b), respectively. It is seen that the measurement approaches to the simulation. The measurement is carried out by Agilent E5071C vector network analyzer. The measured passband insertion losses are about 0.76 dB at center frequency of 2.24 GHz (the 1st measured passband), and about 1.98 dB at center frequency of 3.32 GHz (the 2nd measured passband). The dominant discrepancy of simulation and measurement is central frequency shift, which attributes to the dielectric constant discrepancy and fabrication uncertainty. The dual-band CPW BPF has a miniature circuit size of 40 mm × 5 mm, which is approximately $0.764\lambda_g \times 0.096\lambda_g$, where, λ_g is the guided wavelength at 2.4 GHz.

4.2. Tri-band CPW BPF

A tri-band BPF which centers at 2.4, 3.5 and 5.2 GHz with fractional bandwidth of 14.5%, 7% and 6%, respectively, is also presented, as is shown in Fig. 8(a), and the filter coupling structure is plotted in Fig. 8(b). Where six L-shaped defected patterns introduce six resonances, which are denoted as resonators of R_1, R_2, \dots ,

and R_6 . The coupling coefficients of the neighboring resonators can be calculated as $k_{14} = 0.04$, $k_{25} = 0.07$, $k_{36} = 0.095$. The filter dimensions are obtained as: $l_1 = 11$ mm, $l_2 = 7.3$ mm, $l_3 = 4$ mm, $s_1 = 3.7$ mm, $s_2 = 2.9$ mm, $s_3 = 2.1$ mm, $a_1 = a_2 = 0.2$ mm, $a_3 = 0.1$ mm, $d_1 = 0.4$ mm, $d_2 = 0.8$ mm, $d_3 = 1$ mm.

Simulated filter current distributions are illustrated in Fig. 9. It is noticed that the surface current concentrates on corresponding slot nearby when working at different frequencies, so, it is demonstrated that the triple passbands can be individually controlled by the corresponding etched slots.

The tri-band DCPWS bandpass filter is also fabricated and measured, and the measurement/prediction comparison is illustrated in Fig. 10. The measured passband insertion losses are 1.1 dB, 2.1 dB and 2.7 dB, respectively. The dominant discrepancy between prediction and measurement is also the operation frequency shift, which dominantly attributes to the substrate dielectric discrepancy. The tri-band BPF has the same miniature circuit size as the dual-band BPF.

Comparison of this work and the other related works are listed in Table 3. It can be seen that this work has more flexible design, more operation bands, and even smaller circuit dimensions than the referenced reports.

5. Conclusion

New CPW multi-band bandpass filters with controllable passbands have been developed. For arbitrary passband, the new design has high rejection level at upper stopband. The proposed CPW bandpass filters have simple and compact structures, miniature circuit sizes, controllable center frequencies and bandwidths, and less electromagnetic waves leakiness. The proposed dual-band and tri-band BPFs are fabricated and measured, the experimental results verify the predictions. The proposed CPW filter design scheme is also can be sued for multi-band bandstop filter design.

References

- [1] Shi J, Chen J-X, Xue Q. A quasi-elliptic function dual-band bandpass filter stacking spiral-shaped CPW defected ground structure and back-side coupled strip lines. IEEE Microwave Wireless Compon Lett 2007;17(6):430–2.

- [2] Al-Khateeb L, Abu Safia O. Dual-band bandpass filter based on CPW series-connected resonators. *IET Electron Lett* 2013;49(12):761–2. 269
- [3] Hunga C-Y, Yeb C-S, Yanga R-Y. A compact-size and high isolation dual-band coplanar-waveguide bandpass filter. In: *Proceedings of IEEE MTT-S international microwave symposium, Honolulu, June 3–8; 2007*. p. 925–928. 270
- [4] Schlieter DB, Henderson RM. High Q defected ground structures in grounded coplanar waveguide. *IET Electron Lett* 2012;48(11):635–6. 271
- [5] Marwa Abdel Aziz, Safwat Amr ME, Podevin Florence. Coplanar waveguide filters based on multi-behavior etched-ground stubs. *IEEE Trans Compon Packag Technol* 2009;32(4):816–24. 272
- [6] Hong JS, Lancaster MJ. *Microstrip filter for RF/microwave applications*. New York: John & Wiley Press; 2001. 273
- [7] Zakaria NZ, Mohd Salleh MK, Ismail Khan Z, Abu Hassan AR. Compact coplanar waveguide pseudo-elliptic filter at microwave frequencies. In: *Proceedings of IEEE symposium on industrial electronics & applications (ISIEA), Penang, Malaysia, October 3–5; 2010*. p. 537–540. 274
- [8] Liu HW, Zhang ZC, Wang S. Compact dual-band bandpass filter using defected microstrip structure for GPS and WLAN applications. *IET Electron Lett* 2010;46(21):1444–5. 275

276
277
278

UNCORRECTED PROOF